

This is the peer reviewed version of the following article:

The role of humidity and oxygen on MoS<sub>2</sub> thin films deposited by RF PVD magnetron sputtering / Serpini, Elisabetta; Rota, Alberto; Ballestrazzi, Antonio; Marchetto, Diego; Gualtieri, Enrico; Valeri, Sergio. - In: SURFACE & COATINGS TECHNOLOGY. - ISSN 0257-8972. - 319:(2017), pp. 345-352. [10.1016/j.surfcoat.2017.04.006]

*Terms of use:*

The terms and conditions for the reuse of this version of the manuscript are specified in the publishing policy. For all terms of use and more information see the publisher's website.

14/05/2026 19:02

(Article begins on next page)

## Accepted Manuscript

The role of humidity and oxygen on MoS<sub>2</sub> thin films deposited by RF PVD magnetron sputtering

Elisabetta Serpini, Alberto Rota, Antonio Ballestrazzi, Diego Marchetto, Enrico Gualtieri, Sergio Valeri



PII: S0257-8972(17)30350-X  
DOI: doi: [10.1016/j.surfcoat.2017.04.006](https://doi.org/10.1016/j.surfcoat.2017.04.006)  
Reference: SCT 22249  
To appear in: *Surface & Coatings Technology*  
Received date: 20 September 2016  
Revised date: 8 March 2017  
Accepted date: 4 April 2017

Please cite this article as: Elisabetta Serpini, Alberto Rota, Antonio Ballestrazzi, Diego Marchetto, Enrico Gualtieri, Sergio Valeri, The role of humidity and oxygen on MoS<sub>2</sub> thin films deposited by RF PVD magnetron sputtering. The address for the corresponding author was captured as affiliation for all authors. Please check if appropriate. Sct(2017), doi: [10.1016/j.surfcoat.2017.04.006](https://doi.org/10.1016/j.surfcoat.2017.04.006)

This is a PDF file of an unedited manuscript that has been accepted for publication. As a service to our customers we are providing this early version of the manuscript. The manuscript will undergo copyediting, typesetting, and review of the resulting proof before it is published in its final form. Please note that during the production process errors may be discovered which could affect the content, and all legal disclaimers that apply to the journal pertain.

## The role of humidity and oxygen on MoS<sub>2</sub> thin films deposited by RF PVD magnetron sputtering

Elisabetta Serpini<sup>a,b</sup>, Alberto Rota<sup>c</sup>, Antonio Ballestrazzi<sup>a,c</sup>,

Diego Marchetto<sup>a,b,c</sup>, Enrico Gualtieri<sup>c</sup>, Sergio Valeri<sup>a,b,c</sup>

(a) Dipartimento di Scienze Fisiche, Informatiche e Matematiche - Università di Modena e Reggio Emilia, Via Campi 213/A – 41125 Modena, Italy

(b) Istituto CNR-NANO S3, Via Campi 213/A – 41125 Modena, Italy

(c) Centro Interdipartimentale per la Ricerca Applicata e i Servizi nella Meccanica Avanzata e nella Motoristica Intermech-Mo.Re., Università di Modena e Reggio Emilia, Via Vignolese 905/b-41125 Modena, Italy

**Corresponding author:** Elisabetta Serpini. Telephone: +39 0592055669; Fax: +39 059 2055235  
E-mail: elisabetta.serpini@unimore.it

**Abstract:** MoS<sub>2</sub> is usually applied as thick films (1 μm and above) on sliding counterparts to decrease friction and wear. Thick films of MoS<sub>2</sub> generally grow columnar-like and the bending or fracture of these columns during sliding are supposed to be the origin of the good tribological performances. In the present work, we studied the tribological behavior of 200 nm MoS<sub>2</sub> films prepared by RF magnetron sputtering, with emphasis on the friction mechanisms. We performed ball-on-disc tests at different values of residual humidity, in pure oxygen atmosphere and at different temperatures, in order to disentangle the role of water and molecular oxygen during sliding. We found that, despite the fact that the inner structure of these thin films is not lamellar, the tribological behaviour is similar to thicker ones. The friction in absence of humidity is well below that in standard conditions and the lifetime of the film is strongly enhanced. We observed similar performances in humid air while keeping the sample at 75°C. Our results clearly demonstrated that absorbed water causes the deterioration of the lubricating properties of the films, while film oxidation plays only a marginal role.

**Keywords:** MoS<sub>2</sub>, thin films, PVD, magnetron sputtering, friction

## 1. Introduction

Molybdenum disulfide ( $\text{MoS}_2$ ) is a lamellar solid lubricant, which belongs to the metal dichalcogenides of the form  $\text{MX}_2$ , where M is a metal of oxidation degree 4. Its crystal structure [1] is formed by stacking S-Mo-S tri-layers, in which each Mo atom lies at the center of the triangular prism formed by its six neighboring S atoms to form a  $\text{MoS}_6$  unit. The bonding in the  $\text{MoS}_6$  unit is mainly covalent in nature and thus strong, whereas the S-Mo-S tri-layers are weakly bonded to each other by van der Waals forces. The  $\text{MoS}_2$  conventional unit cell is hexagonal with lattice parameters of  $a=0.316$  nm and  $c=1.229$  nm.

In inert environments and ambient temperature conditions,  $\text{MoS}_2$  and  $\text{MoS}_2$  based composite coatings exhibit exceptional lubricating properties, with reported friction coefficients versus most counterparts in the range of  $10^{-2}$  or less [2-8]. For this reason, molybdenum disulfide has been used since the early Sixties in the aerospace industry [9-13]. These lubricating properties are believed to result from the crystal structure of the material itself, which is lamellar in nature: since the lamellae are separated by weak Van der Waals forces of attraction, they are subjected to easy inter-lamellar shear.

To reach stable ultralow friction, several conditions have to be fulfilled [14-16]. Firstly, adhesion to the substrates should be good, while, at the same time, a transfer film should form on the counterpart [2]. Secondly, the basal planes (0 0 0 1) of  $\text{MoS}_2$  crystallites should be oriented parallel to the sliding direction [2]. Finally, sliding must occur in inert environment or vacuum conditions, since it is well established that oxygen and/or water vapor deteriorate lubricating properties. For example, in an early work from Donnet et al. [2] in which they measured the friction of sputtered  $\text{MoS}_2$  in UHV, HV, dry nitrogen and ambient air, the friction coefficient was found to increase in that order. In addition, Fusaro [17], while investigating rubbed  $\text{MoS}_2$  films in dry argon, dry air and

moist air, found that friction coefficient and wear rate were the highest in moist air, suggesting that water causes the reduction of MoS<sub>2</sub> lubricity.

The obstacles to easy lamellar shear are thought to result from water promoting oxidation and/or water physically bonding to edge sites. In literature, a number of reports support and refute both hypothesis, and a consensus over the prevailing mechanism has not been reached yet. Ross and Sussman [18] were among the first to propose the water-induced oxidation hypothesis, followed by many others during the years [19-21]. They suggested that water oxidizes MoS<sub>2</sub> due to frictional heating in the regions where the asperities come to contact. Oxidation can occur as well at the edge sites during storage in humid environment.

On the other hand, Holinski and Gansheimer [22] hypothesized that friction in presence of water increased not due to oxidation, but to polar bonding between sulfur and water itself, which augmented the shear strength of the material. Windom et al. [23] used Raman spectroscopy on MoS<sub>2</sub> powders to show that a detectable oxide growth only occurred at temperatures above 100°C and that the presence of water had little effect on the system above this temperature. Moreover, tribology tests have shown that friction decreased with increasing temperature in humidity rich environments (humid air, N<sub>2</sub>+H<sub>2</sub>O), while it maintained a stable value in dry conditions (N<sub>2</sub>, N<sub>2</sub>+O<sub>2</sub>) [24]. This is also true in oxygen atmosphere. Recently, Khare et al. [25] investigated the surface contribution of oxidation and moisture to friction of MoS<sub>2</sub> thick films (1 μm) deposited onto steel substrates with a pin-on-flat tribometer. With Energy Dispersive Spectroscopy (EDS) measurements they were able to show that, in humid air at room temperature (RT), the first sliding cycle was sufficient to cause a significant reduction in surface oxygen content due to wear. They observed a further reduction in the twenty subsequent cycles, corresponding to a decrease of the coefficient of friction from 0.2 to 0.12. This means that surface oxides are related to friction, but are quickly removed with wear. This is true for temperatures below 100-150°C, above which the rate of oxides formation prevails upon the rate of oxide removal. The authors also performed annealing in

different atmospheres and EDS measurements showed that no oxidation occurred in humid nitrogen ( $N_2+H_2O$ , no  $O_2$ ), meaning that oxidation only occurs in presence of pure oxygen. Together with their previous results [24], this suggests that water causes an increase of friction at RT without causing oxidation. Further, pump and purge experiments conducted in humid air displayed an instantaneous change in friction with changing environment [26]. These last results seem to contradict the oxidation hypothesis.

Despite the large number of studies on  $MoS_2$ , both experimental and theoretical [27-29], there is still no consensus on whether physisorbed water or water-promoted oxidation is the main cause for the deterioration of  $MoS_2$  friction-reducing properties at RT.

Furthermore, past studies involved coatings prepared in different ways (powder burnishing, CVD, PVD) and of different thicknesses, usually  $1\mu m$  and above, deposited mainly on steel substrates. The selected substrate may have an influence, causing film contaminations that can dramatically modify the tribological properties of  $MoS_2$ . In addition, as reported by some authors, depending on film thickness different crystallites orientation and morphological features may appear [30, 31], driving the tribological properties.

In the early Eighties, Spalvins et al. [10] studied the nucleation and the structure of radio frequency (RF) sputtered  $MoS_2$  films. They found that ultrathin films ( $< 50$  nm) grown at or above RT have a characteristic needle-like ridge pattern, with a crystallite size of 10-15 nm. Between 80 and 200 nm this structure transforms into an equiaxed, dense (pore-free) transition zone. Thicker films grow with a fiber-like structure, with vertical 250 nm wide columns aligned perpendicular to the substrate and separated by pores of a few tens of nanometers. This growth model is widely acknowledged in the scientific community and represents a cornerstone for all the modern studies concerning sputtered  $MoS_2$  films. Spalvins et al. [10] also found that the columns grown above the equiaxed

zone tend to break, so that the actual lubrication is supplied by the 200 nm dense film that remains on the substrate.

In the late Eighties, Fleischauer et al. [3] continued the studies on the structure of sputtered MoS<sub>2</sub> films, confirming the findings of Spalvin et al. [10]. However, for films thicker than 200 nm they found that during sliding the counterpart orientates the crystallites with their basal planes parallel to the sliding direction, so that crystallites shear along the basal planes, with columns rarely fracturing. According to these findings, the whole film contributes equally to the lubrication. For this reason, films thicker than 200 nm have usually been preferred up until now.

In the present work, we prepared thin films (200 nm) by RF magnetron sputtering on Si (111) single crystal covered by native oxide. Our purpose is to study the friction mechanisms of thin films, which do not show a lamellar structure [10]. We focused our attention on thin films because they have not been extensively studied in literature as thicker ones.

We selected Si (111) as substrate in order to minimize contamination from the substrate avoiding the use of an interlayer. For example, an interdiffusive barrier is needed if steel or iron is used as a substrate for MoS<sub>2</sub> deposition, since Sulphur in MoS<sub>2</sub> tends to chemically bond with Iron, thus modifying the lubricating properties of the coating. The choice of substrate also reduces the contribution of surface morphology to the tribological behavior of MoS<sub>2</sub>, as the Si surface has nanometric roughness.

Finally, thin films could be useful in future applications involving MEMS, which are generally made of Si and which cannot employ coatings thicker than a few hundreds of nanometers [32-35]. Moreover, recently Si (111) has attracted special attention as a good mechanical material for MEMS realization [36].

We show that the tribological behavior of thin films is comparable to that of thicker films, which means that other mechanisms, different from the burnishing of the lamellar structure, act in maintaining a low friction coefficient. We ultimately aim to distinguish and clarify the contributions of water and oxygen on the friction properties of these sputter-deposited MoS<sub>2</sub> thin coatings as a function of temperature, which are still debated nowadays, hoping to give further proofs that will end the discussion.

## 2 Methods

MoS<sub>2</sub> coatings were sputter-deposited to a nominal thickness of 200 nm by RF magnetron sputtering technique from a pure MoS<sub>2</sub> target (purity 99.99%). The base pressure of the deposition chamber was 10<sup>-6</sup> mbar. The deposition parameters were the following: 300 W RF power, 0.1 mbar Ar<sup>+</sup> partial pressure, no bias nor sample heating applied. Substrates were Si (111) single crystal 250 mm radius discs, covered with native Si oxide. After the deposition, the coating roughness (RMS) was checked via AFM to be around 1-5 nm. The thickness of the films was estimated by FIB cross-section and varied between 185 nm and 195 nm. The films appeared morphologically featureless both in section and on the surface (see fig. 1), confirming the hypothesis that no columns form below 200 nm thickness [37, 38]. X-Ray Diffraction (XRD) spectra showed weak broad peaks corresponding to (100) and (110) crystallite orientations, which allows us to say that the films are polycrystalline, with crystallites of nanometric size.

The chemical composition of the films was probed with X-ray Photoelectron Spectroscopy (XPS) and Auger Electron Spectroscopy (AES). The chemical homogeneity of the films along the thickness was checked via Auger depth-profiling, acquiring the Mo<sub>MVV</sub>, S<sub>LVV</sub>, O<sub>KVV</sub> and Si<sub>LVV</sub> line emissions during sputtering at 5 keV ion energy and  $\theta = 45^\circ$  incident angle. Fig. 2 shows the corresponding atomic percentage of Mo, S, O and Si versus depth. The first few layers were

composed by atmospheric contaminants (C and H<sub>2</sub>O), which are easily removed in the early stage of sputtering. After contaminants removal, the percentage of S was (53 ± 8)% and that of Mo (36 ± 5)%, where the uncertainty has been calculated as the 15% of the experimental data. This large uncertainty is inherent to the experimental technique employed. From this analysis the film does not seem to be stoichiometric, being S-deficient. However, despite similar results were already reported for MoS<sub>2</sub> deposited by PVD [39], it should also be taken into account that preferential sputtering of the different atomic species can occur. We checked this possibility through a SRIM (Stopping and Range of Ions in Matter) simulation in the case of Ar<sup>+</sup> ions at 3 keV and  $\theta = 45^\circ$  incident angle against Mo and S bulk, which is close to our depth-profiling conditions. From this simulation it follows an atom/ion rate of 3,80 and 3,25 respectively, so there could actually be a preferential sputtering of Mo atoms with respect to S ones, which leads to a lower S/Mo detected signal. Since the simulation was performed considering bulks of Mo and S separately, these results are accurate only supposing that the colliding ions break up the MoS<sub>2</sub> molecule into its constituent atoms, which is a simplification. We can instead exclude an effect of the different escape depth of the involved Auger electrons, since the Auger lines of Mo and S are close to each other in energy and thus the escape depths are comparable. A (10 ± 2 %) percentage of oxygen is present throughout the whole thickness of the film. This value can be considered a standard contamination, presumably due to residual oxygen inside the chamber during the deposition process (in the Results section this hypothesis will be resumed and verified). This value is slightly higher at the surface of the film due to ambient contamination and diminishes in a few sputtering cycles along with the C signal (not reported in figure).

Friction measurements were carried out using a UMT CETR Multi-Specimen Test System placed inside a sealed box mounting a lateral force sensor with a 5-500 mN range in ball-on-disc configuration, at a constant linear velocity of 0.1 m/s and nominal initial load of 400 mN. A precision spindle can rotate the lower specimen at speeds from 0.001rpm up to 5000rpm. The forces

can be measured with a resolution of 0.00003% of the full scale and high repeatability. 100Cr6 balls, 4mm in diameter and with an average surface roughness  $R_a = 30$  nm, were used as the counterpart for tribological tests. In this configuration the initial contact pressure is approximately 430 MPa, estimated applying the Hertzian theory of contact [31, 32]. Tribological measurements were performed in different environments: humid air, dry air, dry nitrogen and dry oxygen (purity of dry  $N_2$  and  $O_2 = 5.0$ ). In the first two instances, a hygrometer, placed near the testing head, was used to estimate the relative humidity inside the sealed box. In the last two cases, no humidity control was employed since tests have been performed in a smaller vessel saturated with dry nitrogen or oxygen, in which a continuous flow of gas was guaranteed during tests. When needed, the samples were back heated during test up to  $75^\circ\text{C}$ . The effective temperature was checked with a thermocouple placed directly on top of the coated discs. A picture of the tribometer has been added in the Supporting Information (Fig. 1). The sealed box, the hygrometer, the smaller container and the heater are indicated.

### 3. Results

According to Khare et al. [24, 25], the frictional behavior of  $\text{MoS}_2$  films is determined by physisorbed water at "low temperature" and by oxidation at "high temperature". The threshold between "low" and "high" depends on the growth procedure. Based on this hypothesis, we performed friction endurance tests at room temperature ( $27 \pm 1^\circ\text{C}$ ) in humid air (65% RH), dry air (8% RH) and dry nitrogen at RT, and at  $75^\circ\text{C}$  in humid air. Illustrative friction curves are plotted versus number of turns in fig. 3.

At RT in humid air (green curve)  $\text{MoS}_2$  exhibited the highest COF and the shortest lifetime. The COF, after an initial 500 turns running-in period, stabilized at 0.17. After approximately  $10^4$  turns, the COF rises up to 0.3, which represents the coating failure, as checked by Auger spectroscopy and

profilometry (see wear profile in Fig. 2a in the Supporting Information). This value was assumed as reference for the other tests in different environments. The lifetime was slightly longer in dry air (light blue curve) at RT. After a running-in period of approximately  $5 \times 10^3$  turns, the COF stabilized at 0.08 for  $10^4$  turns until failure was reached. In nitrogen atmosphere (blue curve) at RT, the coating life doubled with respect to the humid air case and the COF was approximately 0.01, very close to the limit of sensibility of the tribometer ( $5 \text{ mN} / 400 \text{ mN} = 0.0125$ ), for 8 hours, corresponding to  $25 \times 10^3$  turns. The coating did not reach failure, since approximately only half of the coating had been worn away, as highlighted by the wear profile of the track shown in the Supporting Information (Fig. 2b).

From these tests, it is clear that humidity dramatically influences the tribological performances of  $\text{MoS}_2$ . In nitrogen atmosphere (inert environment),  $\text{MoS}_2$  showed a COF ten times smaller than the one obtained in humid air, reaching its best performances. Dry air at RT represented an intermediate case. It should be noted that in dry air the presence of water is drastically reduced (although not eliminated), but oxygen remains.

These results are very similar to those obtained for thicker, lamellar films, although our thin films do not show a lamellar structure. Starting from this similarity, we infer that the oxygen content, which is present in the whole thickness of the film, represents a contamination is not chemically bound to Mo, being just interstitial oxygen. These findings support the thesis that it is the equiaxed 200 nm thick layer which drives the tribological behaviour of PVD  $\text{MoS}_2$  films as proposed by Spalvins et al. [10].

Another way to reduce the presence of water adsorbed at the coating surface is through heating. The chosen heating temperature was reasonably high to induce water desorption without oxidizing the coating, as suggested in several references [23-25]. Friction tests were performed at  $75^\circ\text{C}$  after a thermalization period of 20 minutes. The illustrative measurement reported in fig. 3 (red curve) was

left running for 8 hours, corresponding to  $25 \times 10^3$  turns. In this period the coating did not reach failure and, after the running-in period, it maintained a stable COF value of approximately 0.05. This value was three times lower than the corresponding case at RT and the coating reached a number of cycles similar to the one obtained in nitrogen environment without reaching failure. The annealing of MoS<sub>2</sub> films, beside promoting surface water desorption, might induce out-of-bulk water segregation. As a matter of fact, as found by Khare et al. [25], in humid air water molecules migrate into the film. The stored water in MoS<sub>2</sub> film would increase the interlamellar shear strength, thus increasing friction. Out-of-bulk water segregation could contribute to the COF decrease during annealing.

According to our results, it is mainly the physisorbed water which causes degradation of MoS<sub>2</sub> tribological properties at low temperatures (below 100°C). There is a stark improvement of the tribological performances of the coating with temperature in humid air, where both water and oxygen are present, while no effect was seen in dry environment (air and nitrogen), where the prevalent species are oxygen and nitrogen (see fig. 4). As can be seen from fig. 4, friction curves in dry air (fig. 4a) and in nitrogen (fig. 4b) at RT and at 75°C overlap for the most part. This suggests that no appreciable oxidation, at least due to water molecules, occurs. A complete chemical analysis was not viable since Auger analysis of the tracks which reached failure revealed a preponderance of Si signal with only traces of Mo and S. This is in agreement with wear profiles shown in the Supporting Information and thus with the fact that coating indeed reached failure. A reasonable chemical analysis of the wear track, formed in humid environment, could be performed.

Measurements were done on the debris at the track side. In this case Auger analysis did not evidence an increase of oxygen with respect to the pristine film, suggesting that no oxidation took place. Considering that this is the most severe testing condition in term of oxidation, we do not expect oxide formation in the other cases as well (see Table 1 in Supporting Information). Nothing

certain can be said about oxidation caused by oxygen molecules, since oxygen is present in the first two cases (humid and dry air).

To support the hypothesis that physisorbed water causes degradation of MoS<sub>2</sub> lubricating properties, we carried out a series of tests in humid air by ramping the temperature from RT up to 75°C in three steps (40°C, 55°C, 75°C) and then from 75°C down to RT with the same steps (see fig. 5). All of the tests ran the same number of cycles in order to be comparable in terms of wear of the coating, so that there can be direct comparison between wear track appearance. The same cannot be said for the counterpart, since the number of meters slid by the steel ball is different and related to the radius of the track. Nevertheless, the maximum discrepancy in the number of meters covered was 15%, which we considered acceptable for qualitative considerations.

Since many studies showed that no appreciable increase of the rate of oxidation is induced by temperatures below 100°C [23-25], indicating that the majority of the environmental effect is due to physisorbed humidity, we expected to see a progressive decrease of COF with temperature.

Moreover, we expected the same COF behaviour at the same temperature during heating and cooling steps. On the contrary, if oxidation were the origin of MoS<sub>2</sub> degradation, we would expect to see a different COF at the same temperature during ramping-up and ramping-down, because oxidation is not a reversible process. It is possible that a thin oxide layer forms after each turn and it is quickly worn away with sliding. However, this would not represent the predominant mechanism of MoS<sub>2</sub> degradation. As pointed out by Khare et al. [24, 25], often a single sliding cycle is sufficient to remove this layer so that the COF of the coating is unchanged. The complete tribological test is shown in fig. 5. The first step was in 50% RH humid air at RT (black curve in fig. 5). After a running-in period of 300 turns, the COF reached a steady state value of 0.1, which is typical of MoS<sub>2</sub> rubbed in humid environment [2-8]. The next three steps at increasing temperature (40°C, 55°C and 75°C – light blue, orange and red curves in fig. 5) were almost identical and the COF stabilized at a value close to the lower limit of the sensor sensitivity (below 0.013). Once the

temperature of 75°C is reached, we progressively cooled down the sample to its initial temperature through the same three steps, in order to retrace the heating steps backwards. Above RT (grey and green curve in fig. 5), we found no appreciable differences with respect to the previous heating steps. Finally, going back to RT (blue curve in fig. 5), we retrieved the initial behavior of the COF, which reached a value slightly below 0.1.

Fig. 6 shows the counterpart surface after each test acquired with an optical microscope with a 20x magnification. The temperature at which each test was performed and whether it was during the heating step (fw - forward) or the cooling one (bw - backward) is reported in the picture as well as the corresponding COF measured at the steady state.

It can be seen that, after the first test (RT, fig. 6a), there is transfer film only around the wear scar. The radius of the wear scar is  $R = 140 \mu\text{m}$  and it is the largest of the set. In the heating-up ramp (fig. 6b, 6c and 6d), both the transfer film amount and the radius of the wear scar were smaller, reaching the minimum value of  $R = 70 \mu\text{m}$  in the case of  $T=75^\circ\text{C}$ . The cooling steps in fig. 6e and 6f are very similar to the corresponding heating steps (fig. 6b and 6c). In addition, the appearance of the counterpart at RT in fig. 6g is very similar to that of the first step (fig. 6a). This difference in the resulting wear scars implies that the corresponding contact pressure was not the same throughout all the tests, although the nominal load was kept constant. This fact, however, does not seem to sensibly influence the lifetime of the coating.

These considerations can be extended to the wear tracks appearance (width) as well, as can be seen in fig. 7 (5x magnification). Taking into consideration only the innermost part of the track, thus neglecting the darker borderline, the width of the tracks corresponding to the RT case is approximately  $150 \mu\text{m}$ , which progressively decreases down to  $50 \mu\text{m}$  in the 75°C step. The material removal during hot sliding is very limited, in particular at 55 and 75°C. In this case, the wear tracks are hardly visible at the optical microscope. These features are supported by

profilometric measurements, which also pointed out that at RT the coating was almost worn out (wear depth around 180 nm), while at higher temperatures only few nanometers were worn out. For clarity, we show the comparison between the calculated specific wear rate of the coating and the counterpart for each step in Table 1. The specific wear rate of the coating was calculated taking into account cross-sections of the wear tracks as obtained from profilometry, applied load and number of sliding cycles. The calculation of the counterpart wear rate was performed by modelling the wear cap shape with a standard spherical cap determined from the cap diameter. This is a simplification, since the wear cap is often ellipsoidal in shape (see fig. 6d). The wear cap diameter, calculated as the mean value of parallel and perpendicular dimensions of the wear cap, was estimated from the optical image of the wear scars. From this value and the spherical cap approximation it was possible to calculate the wear volume. In the case of the counterpart the wear rate takes into account the wear volume, load and distance covered by the ball. Data in Table 1 evidence a proportionality between wear and temperature during heating-up and cooling-down, both for the coating and for the counterpart. The only discrepancy from this trend can be found for the wear of the counterpart at RT (fw case). This could be due to the uncertainties related to the estimation of the wear scar and to the many approximations done to perform the calculation in the case of the counterpart.

Step n.	Counterpart Wear Rate [ $10^{-6} \text{ mm}^3/\text{Nm}$ ]	Coating Wear Rate [ $10^{-6} \text{ mm}^3/\text{N}*\text{turns}$ ]
RT (fw)	0.177	43.75
40°C (fw)	0.198	0.85
55°C (fw)	0.027	0.68
75°C	0.007	0.25
55°C (bw)	0.016	0.60
40°C (bw)	0.131	0.65
RT (bw)	1.017	55.50

Table 1: Counterpart and coating specific wear rates at 0.4 N load for every step of the temperature ramp.

The above discussion demonstrates that, below 100°C, heating MoS<sub>2</sub> in humid air does not cause an appreciable increase in the rate of oxidation of the coating with respect to the RT case. This is in agreement with the hypothesis that ambient humidity mainly causes physisorption of water on the MoS<sub>2</sub> surface with no appreciable oxidation of the coating. It is still entirely possible that some degree of oxidation occurs, but to an extent that does not cause deterioration of the tribological properties of the coating, as suggested by Khare et al. [25].

Another set of tests supports these conclusions (fig. 8). Two separate COF measurements were performed in dry nitrogen atmosphere, at room temperature in the first case and at T=75°C in the second one. After an initial run-in period of 10 minutes (approximately 1000 turns), the flux of nitrogen was interrupted for 2 minutes, so that atmospheric air (RH=65%) could enter into the measurement chamber, and restored for one minute. This procedure was repeated 5 times, while we acquired the COF variation. The timing of this procedure was then changed so that the time of permanence in humid air was 5 minutes (repeated 5 times), while keeping fixed to 1 minute the time spent in nitrogen atmosphere for a total of 5 cycles.

Examining the blue curve in fig. 8, corresponding to the RT case, it can be seen that as soon as the nitrogen flux was interrupted, the COF quickly increased from around 0.01 to approximately 0.1, the typical value of MoS<sub>2</sub> in humid air. Even more striking was the abrupt fall to the previous value once the nitrogen flux was restored. At the end of this experiment the coating was not permanently degraded. The COF value reached in humid air in 2 minutes was slightly lower with respect to the corresponding one reached in 5 minutes. This was probably related to the permeability of the chamber to humid air when the nitrogen flux was interrupted, which did not enable the saturation of the volume with humid air. The trend of the COF suggests that, even in 5 minutes, saturation

probably did not take place, because the steady state was not reached. In the high temperature case (75 °C) the COF trend shows some relevant differences. When the time exposure to humid air is 5 minutes, stability is reached and it is possible to discriminate the switch between the two environmental conditions. In this case, the COF in humid air is about one third of that reached at RT, being about 0.3. In this situation the rate of desorption of water molecules increases with respect to that of adsorption, supporting the thesis that below 100°C the physisorbed water drives the frictional behaviour of MoS<sub>2</sub>.

All the results obtained support the hypothesis that, in ambient conditions, absorbed water causes a deterioration of MoS<sub>2</sub>, even in the case of thin films, where MoS<sub>2</sub> crystallites are expected to be randomly oriented [10, 30, 31]. For further validation, we decided to perform a final pump and purge experiment involving pure oxygen (see fig. 9). The tribological test, performed at RT, started in humid air (RH=55%); then, after a running-in period of 15 minutes, pure oxygen was fluxed inside the test chamber for 5 minutes. It can be seen from fig. 9 that the COF dropped from around 0.17 in humid air to 0.02 in pure oxygen. The O<sub>2</sub> flux was then interrupted for 5 minutes, letting humid air in. During that time, the COF grew until it reached the initial value. This cycle was repeated two times with the same results. This procedure was then repeated substituting O<sub>2</sub> with pure N<sub>2</sub> for comparison. It can be seen that fluxing pure N<sub>2</sub> leads to a slightly lower COF with respect to O<sub>2</sub>, about 0.01. Further, two more cycles were performed, in which a dry atmosphere was obtained by equally fluxing pure O<sub>2</sub> and N<sub>2</sub>. This led to an intermediate value of COF with respect to the pure species. Finally, we fluxed alternatively pure O<sub>2</sub> and pure N<sub>2</sub>, 2 minutes each, repeating this cycle two times (see the inset in fig. 9), to highlight the difference between the two ambients. It is confirmed that oxygen leads to a slightly higher COF than nitrogen, with a difference of about 0.01.

This last set of results confirms that O plays a minor role in the tribological behaviour of MoS<sub>2</sub> at RT, causing only a minimal oxidation of the first few layers of the coating (see Table 2), since typical COF value in N<sub>2</sub> is always recovered.

	Mo (%)	S (%)	O (%)	Si (%)	C (%)
Virgin coating	26.0 ± 3.9	63.0 ± 9.5	8.6 ± 1.3	0	2.4 ± 0.4
N <sub>2</sub> /air (RT)	27.1 ± 4.1	55.0 ± 8.3	14.9 ± 2.2	0	3.0 ± 0.5
N <sub>2</sub> /air (HT)	28.7 ± 4.3	40.0 ± 6.0	7.4 ± 1.1	0	23.9 ± 3.6
N <sub>2</sub> /O <sub>2</sub> /air (RT)	25.0 ± 3.8	55.0 ± 8.3	9.8 ± 1.5	0	10.2 ± 1.5

Table 2: Auger surface chemical analysis on the wear tracks before (virgin coating) and after pump and purge tests fluxing N<sub>2</sub> at RT and HT, and N<sub>2</sub>/O<sub>2</sub> at RT. Oxygen content is similar for all tracks within the experimental error.

Finally, to clarify the difference between a “non-oxidized” coating (for which good lubricity is retained) and an oxidized one, we performed ball-on-disc tests after an annealing of 1 hour at 150°C in standard conditions. The results of the tribological tests are displayed in fig. 10. It can be seen that, once the COF stabilizes, there is no difference in the values for humid air or N<sub>2</sub>. Moreover, in both cases the COF value exceeds 0.5. The behavior is distinctly different from what would be expected for one of our standard, “non-oxidized” coating. These differences are evident even from the Auger analysis, revealing a O atomic percentage of about 40% and an almost total lack of S (see Table 3).

Coating	Mo (%)	S (%)	O (%)	Si (%)	C (%)
Non-oxidized	23.6 ± 3.5	40.0 ± 6.0	21.7 ± 3.3	0	14.7 ± 2.2

Oxidized	$43.7 \pm 6.6$	$9.2 \pm 1.4$	$36.3 \pm 5.4$	0	$10.8 \pm 1.6$
----------	----------------	---------------	----------------	---	----------------

Table 3: Surface chemical composition of a non-oxidized and an oxidized coating.

#### 4 Conclusions

MoS<sub>2</sub> has been deposited by RF magnetron sputtering technique onto Si (111) substrates. It is known that its lubricating properties severely degrade in humid air, presumably due to oxidation and/or water physisorption. The aim of the present study was to distinguish the relative roles of water and oxygen in the tribological properties of MoS<sub>2</sub> thin films, where the formation of a columnar structure is not expected [10]. Our results indicate that, even at low film thicknesses (200 nm), the friction properties are strongly dependent to the amount of humidity, which induces the increase of the COF and limits the lifetime of the film. These results support the model proposed by Spalvins et al. [10], who ascribe the tribological behavior of PVD MoS<sub>2</sub> films to the presence of a thin, dense equiaxed layer, which forms in the early stage of deposition. Dedicated tests in different ambient and at different temperatures reveal that at RT it is mainly absorbed water which causes a deterioration of the lubricating properties of the film, while oxygen plays only a marginal role. This is evident from the fact that heating to a temperature slightly higher than RT, but enough for water molecule desorption, greatly improves the tribological properties of the coating. Such values, moreover, are reversible while ramping the temperature up and down, meaning that there is no significant chemical modification of the film (e.g. oxidation). Finally, the exposure of the surface to pure O<sub>2</sub> leads to a very weak increase of the COF with respect to pure N<sub>2</sub> one, still indicating a very limited oxidation of the material at RT. This could be useful in promoting the use of solid lubricants in MEMS/NEMS and high-precision applications where very thin films of controlled thickness are required, since we have shown that to achieve good lubricity there is no need for thick films and wear rate can be controlled and minimized (e. g. through high temperature).

**Acknowledgements**

This work has been supported by Progetto FAR 2014 "Meccanismi di attrito ed usura di superfici autolubrificanti alla multiscala " – Università di Modena e Reggio Emilia, by "MetaGEAR" project – POR-FESR 2014-2020 initiative of Emilia Romagna Region, and by Progetto di Ricerca Applicata 2013/14 – Fondazione Cassa Risparmio Modena N. SIME: 2013.0650. Authors would also like to acknowledge COST Action MP 1303.

ACCEPTED MANUSCRIPT

**References**

1. T. Liang, W. G. Sawyer, S. S. Perry, S. B. Sinnott, S. R. Phillpot, First-principles determination of static potential energy surfaces for atomic friction in MoS<sub>2</sub> and MoO<sub>3</sub>, *Phys Rev. B* 77, 2008, 104-105.
2. C. Donnet, J. M. Martin, T. LeMogne, M. Belin, Super-low friction of MoS<sub>2</sub> coatings in various environments, *Tribol. Int.* 29 (2), 1996, 123–128.
3. P. D. Fleischauer, R. Bauer, Chemical and Structural Effects on the Lubrication Properties of Sputtered MoS<sub>2</sub> Films, *Tribol. Trans.* 31 (2), 1988, 239-250.
4. A.J. Haltner, An evaluation of the role of vapor lubrication mechanisms in MoS<sub>2</sub>, *Wear* 7 (1), 1964, 102-117.
5. V. R. Johnson, G. W. Vaughn, Investigation of the Mechanism of MoS<sub>2</sub> Lubrication in Vacuum, *J. Appl. Phys.* 27 (10), 1956, 1173-1179.
6. X. Ding, X. T. Zeng, X. Y. He, Z. Chen, Tribological properties of Cr- and Ti-doped MoS<sub>2</sub> composite coatings under different humidity atmosphere, *Surf. Coat. Technol.* 205, 2010, 224-231.
7. T. Polcar, A. Cavaleiro, Review on self-lubricant transition metal dichalcogenide nanocomposite coatings alloyed with carbon, *Surf. Coat. Technol.* 206, 2011, 685-695.
8. B. Vierneusel, T. Schneider, S. Tremmel, S. Wartzack, T. Gradt, Humidity resistant MoS<sub>2</sub> coatings deposited by unbalanced magnetron sputtering, *Surf. Coat. Technol.* 235, 2013, 97-107.
9. T. Spalvins, Lubrication with Sputtered MoS<sub>2</sub> Films, *ASLE Trans.* 14, 1971, 267-274.
10. T. Spalvins, A review of recent advances in solid film lubrication, *J. Vac. Sci. Technol. A* 5 (2), 1987, 212-219.
11. L. E. Pope, J. K. G. Panitz, The effects of hertzian stress and test atmosphere on the friction coefficients of MoS<sub>2</sub> coatings, *Surf. Coat. Technol.* 36 (1-2), 1988, 341-350.
12. A. Erdemir, Solid lubricants and self-lubricating films, in: B. Bhushan (Ed.), *Modern Tribology Handbook*, CRC Press, 2001, 787.

13. A. A. Voevodin, J. S. Zabinski, Nanocomposite and Nanostructured tribological materials for space applications, *Compos. Sci. Technol.* 65 (5), 2005, 741-748.
14. M. R. Hilton, P. D. Fleischauer, Applications of solid lubricant films in spacecraft, *Surf. Coat. Technol.* 54-55, 1992, 435-441.
15. A. R. Landsdown, *Molybdenum Disulphide Lubrication*, Tribology Series 35, Elsevier, 1999.
16. N. M. Renevier, J. Hampshire, V.C. Fox, J. Witts, T. Allen, D.G. Teer, Advantages of using self-lubricating, hard, wear-resistant MoS<sub>2</sub>-based coatings, *Surf. Coat. Technol.* 142-144, 2001, 67-77.
17. R. L. Fusaro, *Lubrication and Failure Mechanism of Molybdenum Disulfide Films. I. Effect of Atmosphere*. NASA Technical Paper, 1978.
18. S. Ross, A. Sussman, Surface oxidation of molybdenum disulfide, *J. Phys. Chem.* 59 (9), 1955, 889-892.
19. A.J. Haltner, C.S. Oliver, Effect of water vapor on friction of molybdenum disulfide, *Ind. Eng. Chem. Fundam.* 5 (3), 1966, 348-355.
20. P.D. Fleischauer, Effects of crystallite orientation on environmental stability and lubrication properties of sputtered MoS<sub>2</sub> thin films, *ASLE Trans.* 27 (1), 1984, 82-88.
21. J.K.G. Panitz, L.E. Pope, J.E. Lyons, D.J. Staley, The tribological properties of MoS<sub>2</sub> coatings in vacuum, low relative humidity, and high relative-humidity environments, *J. Vac. Sci. Technol. A -Vac. Surf. Films* 6 (3), 1988, 1166-1170.
22. R. Holinski, J. Gansheimer, A study of the lubricating mechanism of molybdenum disulfide. *Wear* 19 (3), 1972, 329-342.
23. B.C. Windom, W.G. Sawyer, D.W. Hahn, A Raman spectroscopic study of MoS<sub>2</sub> and MoO<sub>3</sub>: applications to tribological systems, *Tribol. Lett.* 42 (3), 2011, 301-310.

24. H.S. Khare, D. L. Burris, The effects of environmental water and oxygen on the temperature-dependent friction of sputtered molybdenum disulfide, *Tribol. Lett.* 52 (3), 2013, 485–493.
25. H.S. Khare, D. L. Burris, Surface and Subsurface Contributions of Oxidation and Moisture to Room Temperature Friction of Molybdenum Disulfide, *Tribol. Lett.* 53 (1), 2014, 329–336.
26. R.S. Colbert, The Role of Water on the Tribological Properties of Molybdenum Disulphide Films. Doctoral Dissertation, University of Florida, Gainesville, 2012.
27. G. Levita, A. Cavaleiro, E. Molinari, T. Polcar, M. C. Righi, Sliding Properties of MoS<sub>2</sub> Layers: Load and Interlayer Orientation Effects, *J. Phys. Chem. C* 118, 2014, 13809–13816.
28. T. Liang, W. G. Sawyer, S. S. Perry, S. B. Sinnott, S. R. Phillpot, First-Principles Determination of Static Potential Energy Surfaces for Atomic Friction in MoS<sub>2</sub> and MoO<sub>3</sub>. *Phys. Rev. B* 77, 2008, 104105–104110.
29. L. Hromadová, R. Martonák, E. Tosatti, Structure Change, Layer Sliding, and Metallization in High-pressure MoS<sub>2</sub>. *Phys. Rev. B* 87, 2013, 144105–144110.
30. T. Spalvins, Morphological and frictional behavior of sputtered MoS<sub>2</sub> films, *Thin Solid Films* 96 (1), 1982, 17–24.
31. V. Buck, Morphological properties of sputtered MoS<sub>2</sub> films, *Wear* 91 (3), 1983, 281–288.
32. S. Lee, S. Park, D. Cho, A new micromachining technology using (111) silicon, *Japan. J. Appl. Phys.* 38, 1999, 2699–2703.
33. J. A. Williams, *Engineering Tribology* 488, Cambridge University Press, 2005.
34. A. Savan, E. Pfluger, P. Voumard, A. Schroer, M. Simmonds, Modern solid lubrication: recent developments and applications of MoS<sub>2</sub>, *Lubri. Sci.* 12, 2000, 185–203.
35. S. Yong, K. Sang-Gook, A lateral, self-cleaning, direct contact MEMS switch, in: *Micro Electro Mechanical Systems 2005, MEMS 2005, 18<sup>th</sup> IEEE, International Conference on 30 January – 3 February 2005, 2005*, 195–198.

36. J. Kim, D. Cho, R. S. Muller, Why is (111) silicon a better mechanical material for MEMS?, in: E. Obermeier (Ed.), Transducers '01 Eurosensors XV, Springer- Verlag Berlin Heidelberg, 2001, 662-665.
37. T. R. Jervis, M. Nastasi, R. Bauer, P. D. Fleischauer, Laser surface processing of Molybdenum Disulfide thin films, Thin Solid Films 181, 1989, 475-483.
38. J. Wang, W. Lauwerens, E. Wieers, L. M. Stals, J. He, J. P. Celis, Structure and tribological properties of MoS<sub>x</sub> coatings prepared by bipolar DC magnetron sputtering, Surf. Coat. Technol. 139, 2001, 143-152.
39. H. Dimigen, H. Hubsch, P. Willich, K. Reichelt, Stoichiometry and Friction Properties of Sputtered MoS<sub>x</sub> layers, Thin Solid Films 129 (1-2), 1985, 79-91.
40. K.L. Johnson, Contact Mechanics, Cambridge University Press, Cambridge, 1999.
41. K. L. Johnson, One hundred years of Hertz contact, Proceedings of the Institution of Mechanical Engineers 196, 1982, 363– 378.

**List of figures captions**

Fig. 1. SEM images of 200 nm MoS<sub>2</sub> coatings: (a) top view, magnification 50kx; (b) cross-section, magnification 150kx.

Fig. 2. Typical depth profile of MoS<sub>2</sub> coatings. Sulphur, Molybdenum, Oxygen and Silicon signal are reported (Carbon not shown).

Fig. 3. Friction endurance tests at RT in humid air (green curve), dry air (light blue curve) and N<sub>2</sub> atmosphere (blue curve), and at 75°C in humid air (red curve).

Fig. 4. Comparison between friction endurance tests in (a) dry air at RT and HT, and (b) in N<sub>2</sub> at RT and HT.

Fig. 5. Temperature ramp experiment: friction curves.

Fig. 6. Optical microscope images (20x magnification) of the counterpart acquired after each heating (fw) or cooling (bw) step in the temperature ramp experiment. The corresponding COF is reported for each step.

Fig. 7. Optical microscope images (5x magnification) of the wear tracks corresponding to the temperature ramp experiment, from the heating-up steps (forward, fw) to the cooling (backwards, bw) ones.

Fig. 8. Pump and purge experiments in N<sub>2</sub> at RT (blue curve) and at 75°C (red curve).

Fig. 9. Pump and purge experiment in pure O<sub>2</sub>, pure N<sub>2</sub> and a mix of the two gases. The corresponding gas flux is specified in the bottom part of the graph. The enlarged portion of the COF vs time graph highlights the small difference between N<sub>2</sub> and O<sub>2</sub> flux in terms of friction.

Fig. 10. Friction vs distance in humid air (black curve) and N<sub>2</sub> (red curve), both at RT, for an oxidized coating.

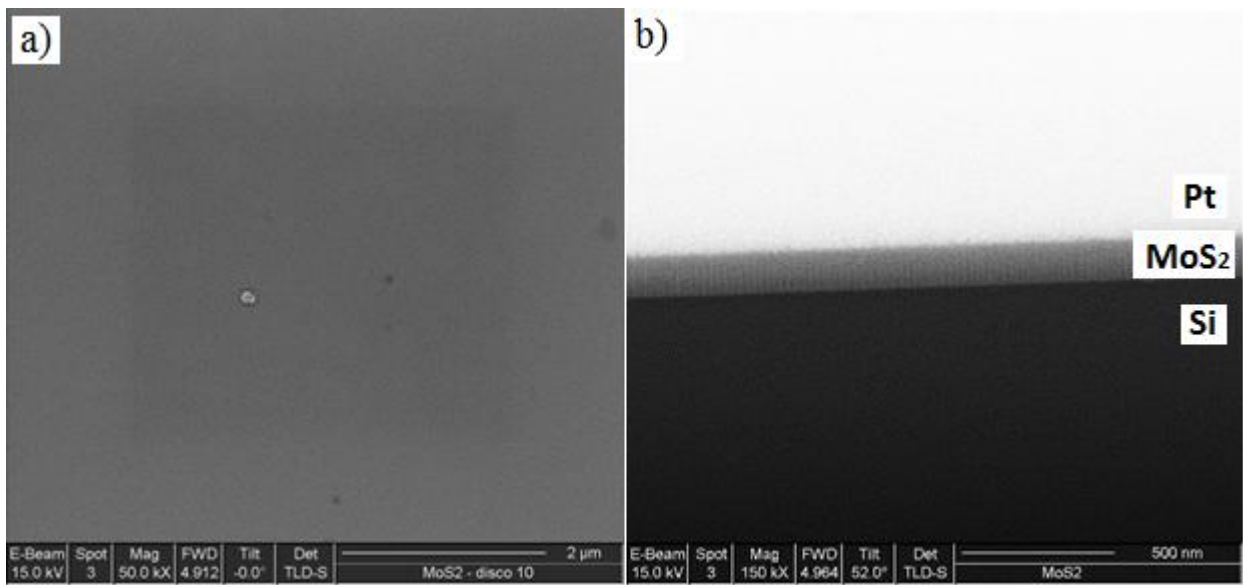


Figure 1

ACCEPTED MANUSCRIPT

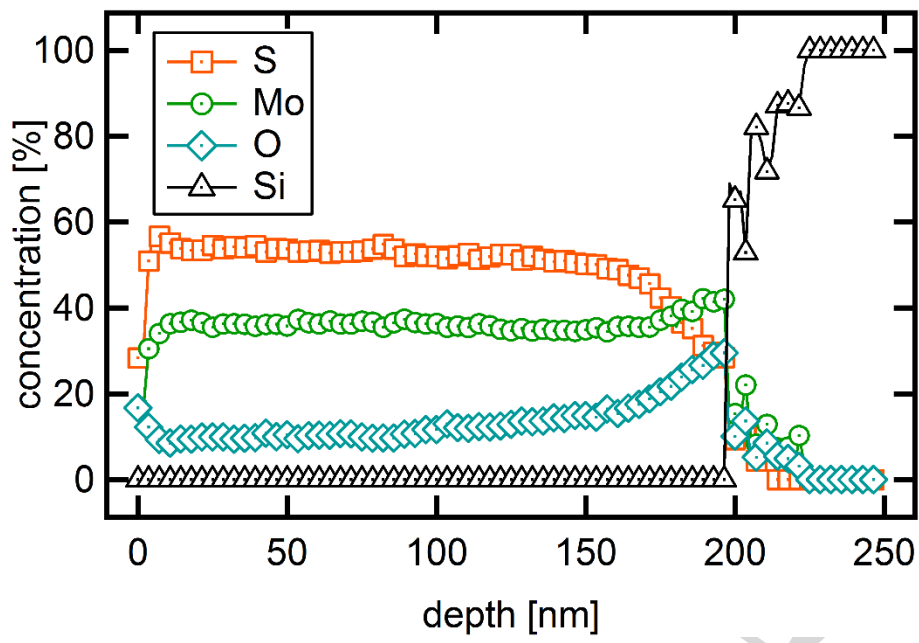


Figure 2

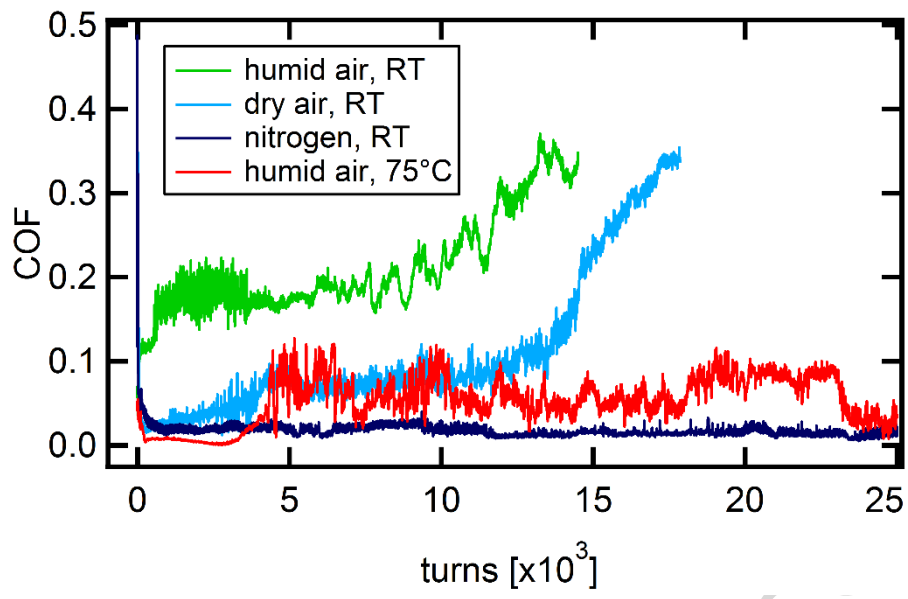


Figure 3

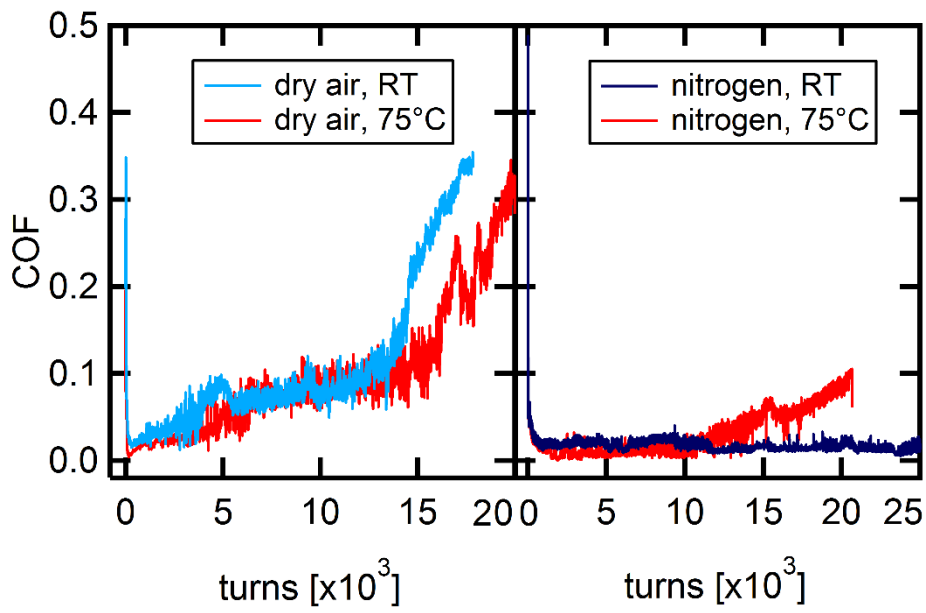


Figure 4

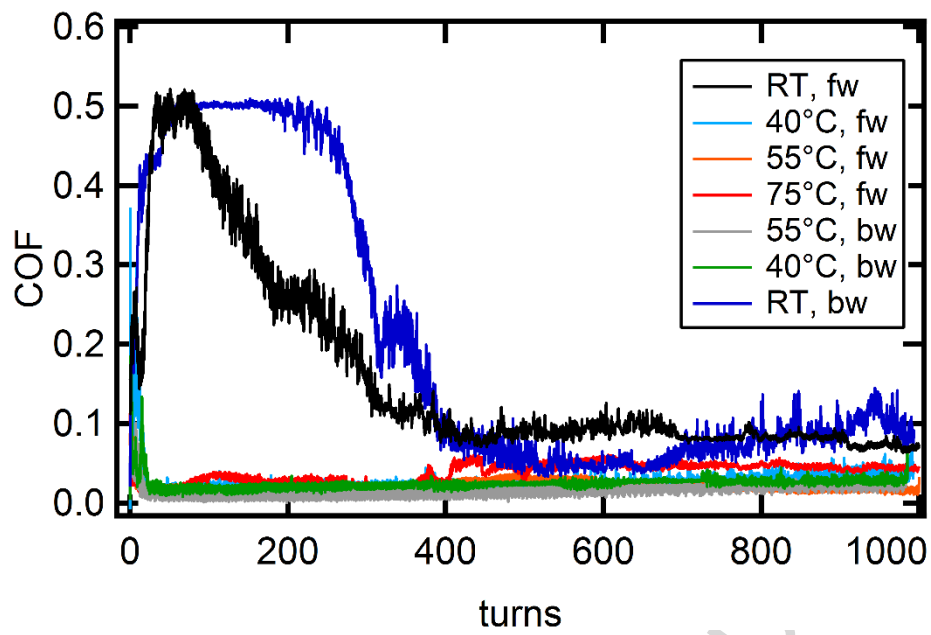


Figure 5

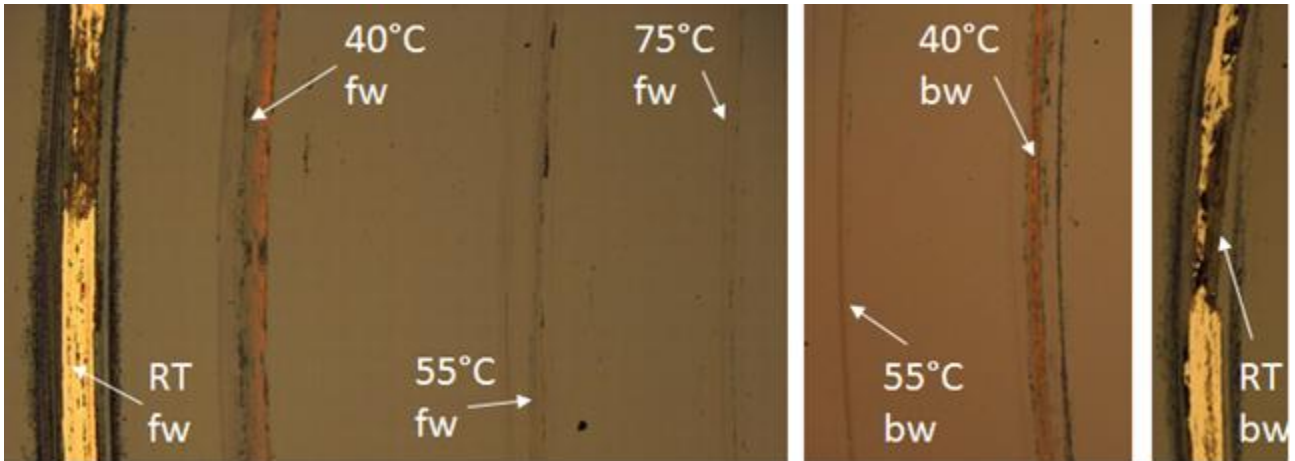


Figure 6

ACCEPTED MANUSCRIPT

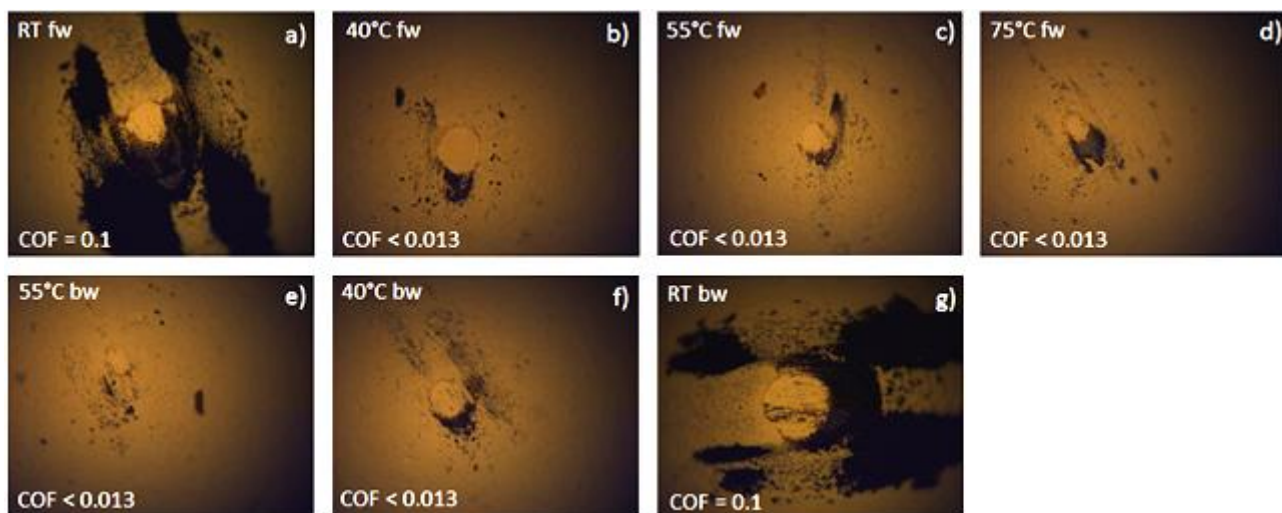


Figure 7

ACCEPTED MANUSCRIPT

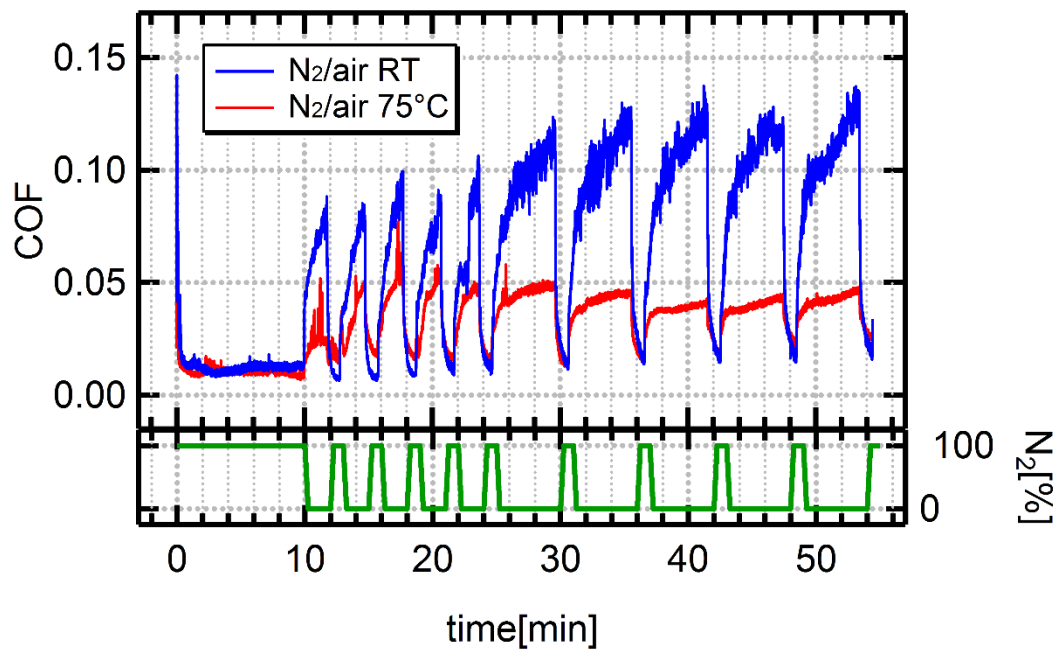


Figure 8

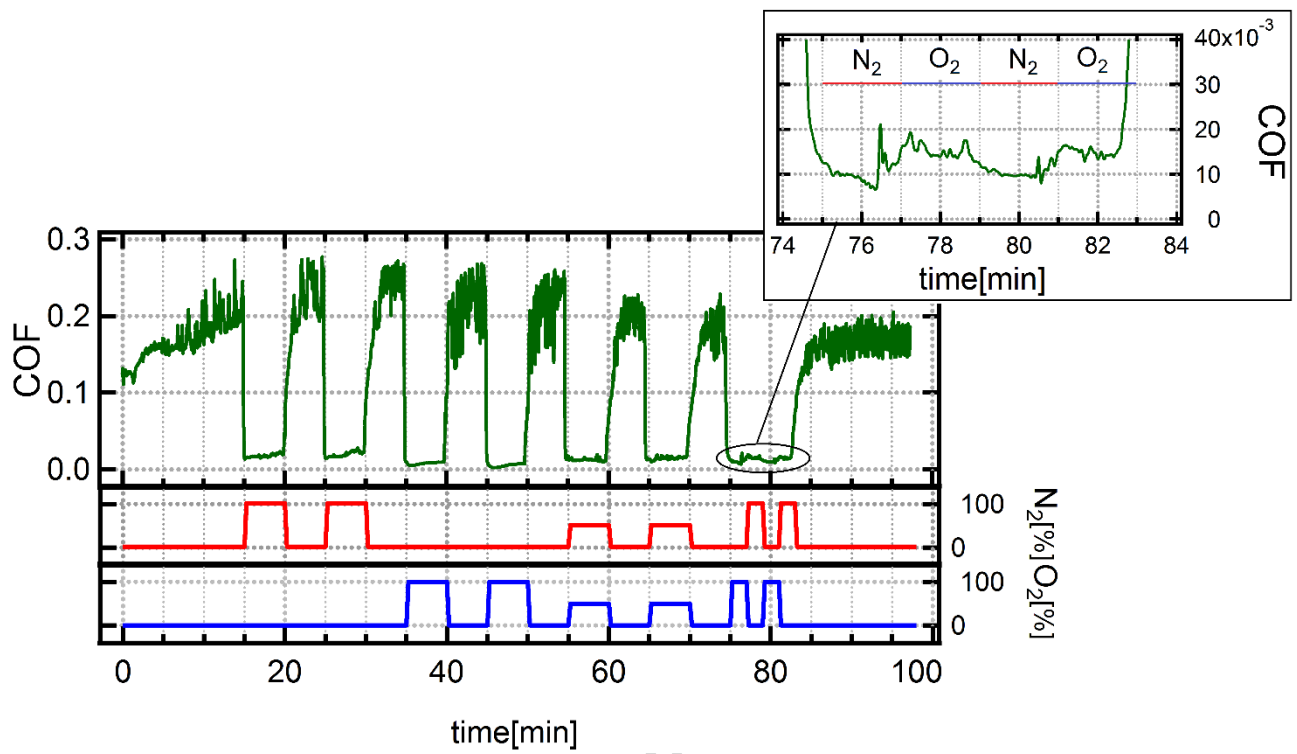


Figure 9

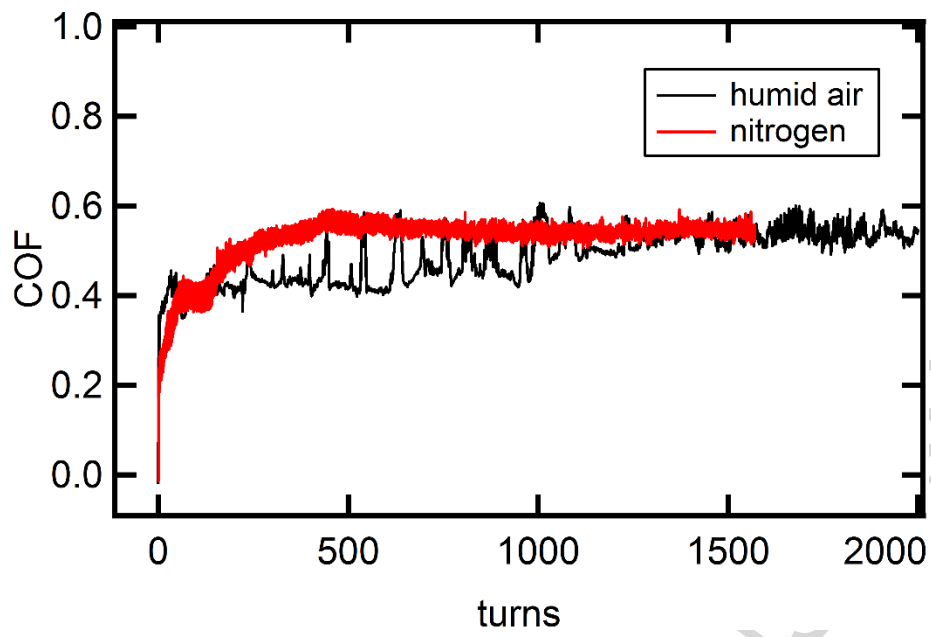


Figure 10

**Highlights**

Thin quasi-amorphous MoS<sub>2</sub> films were grown by RF magnetron sputtering technique.

200 nm amorphous MoS<sub>2</sub> films show the same tribological behavior as thicker ones.

Friction and wear are lower in humidity-free ambient and/or at T above 40°C.

At RT adsorption of water molecules increases the shear strength between MoS<sub>2</sub> planes.

At RT oxidation of the film plays a marginal role.

ACCEPTED MANUSCRIPT